BELLCOMM, INC.

SUBJECT: Comparison of Sensor Performance and Initial Error Covariance Matrices for Rendezvous Navigation - Case 310

DATE: December 18, 1968

FROM: W. O. Covington

TM-68-2014-6

TECHNICAL MEMORANDUM

I. INTRODUCTION

The rendezvous radar aboard the LM and the sextant and VHF ranging device aboard the CM are sensors which can provide data for lunar orbit rendezvous navigation. A comparison of the navigation performance of the Kalman filter when using these sensors individually and in combination is presented in this memorandum. Specific questions of interest are: What measurement errors are tolerable for the VHF ranging device? and What covariance matrix should be used to initialize the Kalman filter? The Bellcomm Statistical Error Simulation Program[1] was used to compute the performance of the Kalman filter working with the various navigation sensors and initial error covariance matrices.

II. RENDEZVOUS TRAJECTORY

The lunar orbits used in this analysis for the CM and the LM were specified by MSC for the Abort Guidance System (AGS) performance analysis purposes;[2] the trajectories can be summarized as follows:

1. CSM is in a 60 NM circular orbit,
2. LM inserts into a 9.85 x 30 NM elliptical orbit coplanar with CSM,
3. Phase angle at insertion is 23.95 deg., CSM ahead of LM,
4. CSI occurs 30 minutes after insertion,
5. CDH occurs at first apsis.

The statistical simulation was begun at CSI time and was terminated at an arbitrary time 3060 sec. later. A 30 NM differential altitude between CSM and LM orbit after

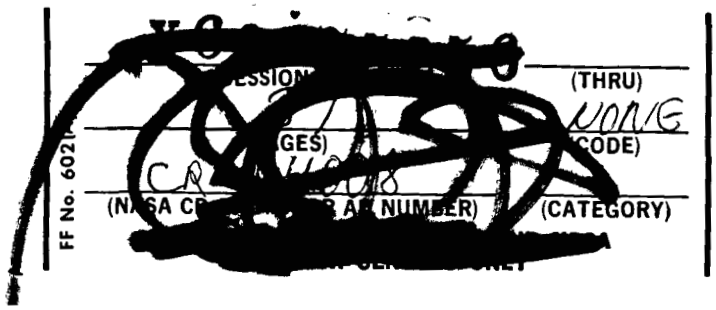

CDH resulted from not making a CSI burn and from circularizing the LM orbit one-half period after insertion. The CDH maneuver was made at the 30 NM apoapsis of the LM trajectory, 1555 sec after CSI time; Figure 1 displays LM altitude and relative position and velocity.

Navigation marks were begun 3 minutes after CSI and were continued subsequently at 4-minute intervals. An examination of the effects of the measurement schedule on navigation performance was not included in this analysis.

No maneuvers were made based on the navigation information. The CDH maneuver was precomputed and the required ΔV and time of CDH inserted into the program as input data. A nominal and perfect CDH was made without execution error.

III. BELLCOMM STATISTICAL ERROR PROGRAM

The estimated covariance matrix, $\hat{E}$, of the navigation error, $\underline{e}$, (Figure 2) is computed by the Kalman filter algorithms[3] implemented in the Bellcomm Statistical Error Simulation Program. The actual navigation error covariance matrix, E, which forms the output of this study, is computed from the estimated covariance matrix as shown in Appendix 1.

It should be emphasized that the actual covariance matrix computed by this program is a statistical representation of the actual navigation error expected for an ensemble of trajectories. The error sources which contribute to the actual covariance matrix are the initial actual error covariance matrix and the subsequent actual measurement errors of the sensors. The estimated covariance matrix, on the other hand, is initially a set of numbers (for starting the Kalman filter) which may or may not be an accurate estimate of the actual error. Subsequently, the estimated covariance matrix is determined by the initial covariance matrix estimate and the estimate of the measurement errors of the sensors.

It should be pointed out that this study dealt with relatively small navigation errors in which the linearity assumption of the statistical simulation was surely not violated. Implicit in the Kalman filter algorithms is the assumption that the measurement deviation vector is linearly related to the state deviation vector. Substantially larger navigation errors which violate this linearity assumption would require a Monte Carlo simulation rather than the statistical simulation. The results of statistical simulation program computations would not reveal a linearity assumption violation, if there were one, unless the results were compared with the results of a Monte Carlo simulation.

The results of the study are presented as root-sum-square (RSS) position and velocity errors derived from the actual error covariance matrix $E = \varepsilon(\underline{e}\ \underline{e}^T)$. Let the navigation error have position and velocity vector components

$$\underline{e} = \begin{pmatrix} \underline{e}_x \\ \underline{e}_v \end{pmatrix}$$

where

$\underline{e}_x$ = position error vector

$\underline{e}_v$ = velocity error vector

The RSS position and velocity error respectively are defined as:

$$RSS_x = \sqrt{tr\ \varepsilon(\underline{e}_x \underline{e}_x^T)}$$

$$RSS_v = \sqrt{tr\ \varepsilon(\underline{e}_v \underline{e}_v^T)}$$

where ε is the expectation operator

IV. CASES RUN

Cases were selected and run to assess the effect on navigation performance of the initial estimated E-matrix and of navigation sensor errors. The initial actual E-matrix, E, was in all cases taken to be an "MSFN E-matrix" representing LM state uncertainties after MSFN tracking of the LM between insertion and CSI. Four sets of cases were run, each with different initial estimate E-matrices, $\hat{E}$, shown in Table I. These covariance matrices are expressed in LM local vertical coordinates (up, forward, cross-plane) as follows:

$$
\begin{array}{cccccc}
\sigma_{X(up)} & & & & & \\
\rho_{XY} & \sigma_{Y(fwd)} & & & & \\
\rho_{XZ} & \rho_{YZ} & \sigma_{Z(cross)} & & & \\
\rho_{X\dot{X}} & \rho_{Y\dot{X}} & \rho_{Z\dot{X}} & \sigma_{\dot{X}(up)} & & \\
\rho_{X\dot{Y}} & \rho_{Y\dot{Y}} & \rho_{Z\dot{Y}} & \rho_{\dot{X}\dot{Y}} & \sigma_{\dot{Y}(fwd)} & \\
\rho_{X\dot{Z}} & \rho_{Y\dot{Z}} & \rho_{Z\dot{Z}} & \rho_{\dot{X}\dot{Z}} & \rho_{\dot{Y}\dot{Z}} & \sigma_{\dot{Z}(cross)}
\end{array}
$$

where

σ_X, σ_Y, σ_Z are position standard deviations in thousands of feet

$\sigma_{\dot{X}}$, $\sigma_{\dot{Y}}$, $\sigma_{\dot{Z}}$ are velocity standard deviations in feet per second

ρ_{ij} are correlation coefficients

The results with Matrix (1), the MSFN E matrix, represent the navigation errors associated with a best estimate initial covariance matrix. Matrix (2), consisting of only the diagonal elements of Matrix (1), shows the effect of simplifying the initial covariance matrix by zeroing the correlation terms. Matrix (3), which is further simplified from Matrix (2), has the same RSS position and velocity errors as Matrices (1) and (2) except that the errors are equally apportioned in the three directions. Matrix (4) has twice the RSS position and velocity errors as Matrix (3) and shows the effect of changing the error magnitudes of the scalar diagonal initial E-matrix. The names associated with the matrices in Table I are used in Figures 3 through 10.

Cases run for each of the four sets consisted of the following sensor combinations:

1. VHF only, 1 σ = 80 ft. (nominal VHF)
2. VHF only, 1 σ = 240 ft. (degraded VHF)
3. VHF only, 1 σ = 500 ft. (degraded VHF)
4. VHF only, 1 σ = 1000 ft. (degraded VHF)

5. SXT-only

6. SXT + VHF

7. PNGCS (Rendezvous Radar)

The 80 ft 1σ for VHF corresponded to an accepted estimate of the expected performance of the VHF.[4] The other three VHF-only cases show the effect of degraded VHF performance. A recent estimate of the VHF ranging performance based on test data is 3σ = 424 ft.[5] The performance associated with this error can be seen by interpolating the curves of the results.

V. SENSOR ERRORS

The values of the undegraded 1σ sensor errors used in the simulation are listed in Table II with the sources referenced. These values were derived from the rendezvous radar specifications, the PNGCS and AGS P & I specifications, and from estimates of VHF performance. Whereas the Bellcomm statistical computer simulation does not estimate measurement error biases, both bias and random errors attributed to the PNGCS sensors were root-sum-squared and used as random errors in this simulation.

We feel that the present study method of using a larger PNGCS angle random error (larger because it is the RSS of the actual random error and the angle bias) gives comparable results (in RSS navigation error) to the use of a smaller angle random error and simultaneous estimation of the angle biases. In the present study, the weights from the Kalman filter algorithm are low, because of the large instrument error variance. In the PNGCS, the weights on the state vector are also low, despite the smaller instrument error variance, because the angle bias must also be estimated as well as the state vector. Further support for this approach is contained in Appendix B to the AGS improved radar filter study.[8]

VI. INITIAL COVARIANCE MATRIX

The initial LM actual error covariance matrix used in the study represents the accuracy with which the state of the LM can be determined using data from the MSFN. This matrix was one of several published by MPAD in June 1967 for studies of AGS-controlled ascent to rendezvous.[9] These matrices corresponded to LM equatorial launch sites from 45°E to 45° W longitude. The covariance matrix corresponding to the 0° launch site was selected for this study since its RSS position and velocity error magnitudes are typical of all sites except the westerly launch sites.

Especially large errors are associated with the westerly launch sites since there is less time for MSFN tracking and orbit determination after LM insertion. The MSFN tracking arc upon which the covariance matrix is based extends from launch burnout to either the time of CSI minus 10 minutes or LM occultation minus 10 minutes, whichever occurs first.

The ten minute interval was allowed for orbit determination convergence, update, and pre-thrust program between the last usable MSFN data and either the CSI maneuver or LM occultation, whichever was earlier. The covariance matrix as presented by MPAD was referenced to an epoch at ascent burnout, but represented the uncertainty in the LM state at epoch time based on the permissible MSFN tracking data between insertion and CSI.

This covariance matrix may not be the most recent estimate of MSFN capability, although it is felt that the relative navigation performance using different navigation sensors as presented in this report will remain unchanged.

VII. DISCUSSION OF RESULTS

The rendezvous navigation performance for various sensors and initial estimated E-matrices is compared in Figures 3 through 10. The figures show RSS position and velocity errors derived from the actual (not the estimate) state vector covariance matrix. A "no nav" curve is also included which shows the propagation of initial errors associated with the MSFN E matrix. RSS errors both before and after making navigation calculations are shown in the figures; the constant time portions of the curves indicate the reduction in RSS error afforded by each navigation measurement.

The following chart is a useful guide to the figures.

E-Matrix	Position Error	Velocity Error
MSFN E	Fig. 3	Fig. 4
Diagonal MSFN E	5	6
Scalar Diagonal MSFN E	7	8
2x Scalar Diagonal MSFN E	9	10

From these figures it can be observed that the VHF-only performance tends to follow the "no nav" curves, except the case in Figures 3 and 4 where the MSFN E-matrix is used as an initial estimated E-matrix. Only during limited time intervals (between 1600 sec and 2300 sec in Figures 5 and 7, for example) does the VHF only, when initialized by a diagonal E-matrix, offer substantially lower errors than "no nav".

The reason for this somewhat surprising result can be understood by comparing local vertical component curves of the VHF-only error with corresponding components for "no nav". These curves, which are presented in Figures 11-14, show that the navigation performance with VHF-only measurements is dominated by the out-of-plane error. As would be expected, the VHF reduces the forward or downrange position error significantly. Comparison of the up-direction curves show that the VHF actually increases the up-direction position error. The major capability of the VHF ranging is to reduce in-plane errors. Since the cross-plane error was dominant for the MSFN E matrix used in this analysis, the VHF measurements were of little benefit unless initial correlations were introduced in the initial estimated E-matrix between the in-plane and out-of-plane errors. The state transition matrix does not build up correlation between the in-plane and out-of-plane error components.

The actual navigation error as presented in Figures 3 through 10 is distinctly different from the estimate navigation error as generated by the Kalman filter algorithm. Figures 15 and 16, which illustrate these errors for 1σ = 80 ft VHF-only show that the actual error in this case was, at some times, a factor of two larger than the Kalman filter estimates. The differences between the actual and estimated covariance matrices arise from the difference between the initial actual and estimated E-matrices and from the difference between the actual and estimated measurement error covariance. The relationship between these factors can be seen in Eq. (9) of Appendix 1. In this analysis the sensor actual and estimated error covariances were identical, so that the difference between the actual and estimated covariance matrices arose from the differences in their initial values.

The SXT-only performance is much better than the VHF-only performance, as can be seen in Figures 3 through 10. The SXT-only immediately reduces the out-of-plane error component and continues to constrain it, whereas this component is not altered by the VHF-only and dominates its RSS error. The operational use of the SXT for rendezvous navigation may be somewhat limited, however, since there may not be sufficient light contrast between the LM and the moon background except for brief periods when the sunlit LM is viewed against the moon either in darkness or lighted by earthshine, or when the LM's flashing light is distinguishable.

Although the VHF in conjunction with the SXT reduces the navigation error even lower than for SXT-only (Figures 3-10), the further reduction afforded by the VHF provides marginal benefit. On the other hand, the addition of SXT measurements to VHF measurements provides a marked improvement in performance. Even one SXT mark would be very beneficial, since it would reduce the out-of-plane position error.

The effectiveness of optical measurements in reducing out-of-plane position error suggests that VHF measurements should be augmented with optical measurements with the Crew Optical Alignment Sight (COAS) if the sextant is unavailable. At the initial range of 1.7×10^6 ft, the 9000 ft out-of-plane error of this analysis corresponds to an angle of 5 mr. Hence, if the measurement error of the COAS were about 5 mr or less, it would be desirable to include some COAS measurements to reduce the out-of-plane error which is not altered by the VHF. Figs. 17 and 18 show the improvement made by augmenting the VHF with 3 COAS marks.

The navigation performance using different initial estimated E matrices for PNGCS is summarized in Figures 19 and 20. Since the position and velocity errors for MSFN E are substantially less than those for scalar diagonal E, it seems desirable to use the MSFN E matrix as an initial estimate rather than a somewhat arbitrary scalar diagonal matrix. Use of the MSFN E would, of course, require the transmission of the elements of MSFN E from the ground to the LM. Overlay restrictions in erasable memory may limit the time intervals during which the covariance matrix could be uplinked. The covariance matrix storage registers are shared by other programs and routines, and conflicts must be avoided. While program modifications could surely alleviate these practical problems, the existing overlay restrictions may permit uplinking the MSFN E. If the non-diagonal MSFN E cannot be implemented, the figures show that the next best thing to do is uplink the diagonal elements of the MSFN E. The currently planned technique of using a scalar diagonal initial covariance matrix is the least desirable of the three. Doubling the RSS position and velocity errors of the scalar diagonal matrix does not have much effect on the results.

A set of curves comparing various levels of VHF performance is displayed in Figures 21 and 22. Subjective comparison of the curves shows that a VHF-only 1σ = 500 ft is approximately comparable to PNGCS. This conclusion applies only for the curves illustrated in the figures where MSFN E is used as the initial estimated E-matrix, since VHF-only does not substantially improve navigation performance over "no nav" when the initial estimated E is taken to be a diagonal matrix.

VIII. CONCLUSIONS AND RECOMMENDATIONS

Based on the results of this study, the following recommendations can be made:

1. When using VHF-only data, the MSFN E-matrix (or some other best estimate non-diagonal covariance matrix) should be used as an initial estimated E-matrix.

2. The smaller errors resulting from sextant-only make it a more desirable sensor than VHF-only. There is marginal benefit in augmenting sextant measurements with VHF measurements.

3. To greatly reduce the out-of-plane errors, VHF measurements should be augmented with one or more sextant marks. If sextant operation is not possible, COAS measurements would be a desirable addition to the VHF.

4. Either the MSFN E or the diagonal MSFN E Matrix yields smaller errors with the PNGCS than a scalar diagonal initial E-matrix. If a scalar diagonal matrix is used, a factor of two difference in the scalar factor makes little difference in the subsequent error.

W. O. Covington

2014-WOC-bjw

Attachments
Appendix 1
Figures 1 - 22
References
Tables 1 and 2

REFERENCES

1. Bellcomm memorandum by W. G. Heffron, "Statistical Error Simulation Program Equations - Case 310", 14 Oct 68

2. Enclosure 2 to MSC letter EG43-247-68-386, "PNGCS/AGS Performance Analysis Comparison Meeting", 9 April 68.

3. Battin, Astronautical Guidance, Chapter 9, McGraw-Hill, 1964

4. Conversation with K. H. Schmid of Bellcomm, 4 April 1968.

5. Conversation with K. H. Schmid of Bellcomm, 12 September 68.

6. MSC Internal Note No. 68-FM-17, "Navigation Capabilities of the Sextant and Ranging Device for CSM-Active Rendezvous," 18 January 68.

7. Enclosure 1 to letter of Reference 2.

8. TRW 05952-6214-T000, LM/AGS Radar Filter Improvement Feasibility Study, June 68.

9. Attachment to MSC memorandum 67-FM46-125, "MSFN support of AGS Rendezvous," 14 June 67.

APPENDIX 1

DERIVATION OF ACTUAL COVARIANCE MATRIX OF NAVIGATION ERROR

The basic equations of the Kalman Filter are (see Figure 2):

$$\hat{E}_+^{-1} = \hat{E}_-^{-1} + H\hat{Q}^{-1}H^T \tag{1}$$

$$W = \hat{E}_+ H\hat{Q}^{-1} = \hat{E}_- H(H^T\hat{E}_- H + \hat{Q})^{-1} \tag{2}$$

$$\hat{x}_+ = \hat{x}_- + W(\alpha - H^T e_-) = \hat{x}_- + W(\tilde{q} - \hat{q}) \tag{3}$$

$\hat{E}_+$ = estimated covariance matrix of navigation error, e, after incorporating navigation data

$\hat{E}_-$ = estimated covariance matrix of navigation error, e, before incorporating navigation data

H = measurement sensitivity matrix

$\hat{Q}$ = estimated measurement error covariance matrix

W = weighting matrix of filter

α = measurement error

e_- = navigation error prior to incorporating measurement, (see Figure 2)

$\hat{x}_-$ = estimated state vector prior to incorporating measurement data (see Figure 2)

$\hat{x}_+$ = estimated state vector after incorporating measurement data (see Figure 2)

$\tilde{q}$ = instrument reading

$\hat{q}$ = expected instrument reading

From the definitions of Figure 2,

$$\delta\hat{x}_+ = e_+ + \delta x, \tag{4}$$

$$\delta\hat{x}_- = e_- + \delta x. \tag{5}$$

Substituting equations (2), (4), and (5) in Equation (3),

$$e_+ = e_- + \hat{E}_+ H\hat{Q}^{-1} \alpha - \hat{E}_+ H\hat{Q}^{-1}H^T e_- \tag{6}$$

Substituting equation (1) into equation (6),

$$e_+ = \hat{E}_+ H\hat{Q}^{-1} \alpha + \hat{E}_+\hat{E}_-^{-1} e_- \tag{7}$$

The actual covariance matrix of the navigation error in terms of the estimated covariance matrix is:

$$E = \varepsilon(e_+ e_+^T) \tag{8}$$

$$E = \hat{E}_+(H\hat{Q}^{-1}Q\hat{Q}^{-1}H^T + \hat{E}_-^{-1}E_-\hat{E}_-^{-1})\hat{E}_+ \tag{9}$$

where ε denotes the expectation operation.

Equation (9) is used in the Bellcomm simulation program to compute the actual error covariance matrix of the navigation error in terms of the estimated covariance matrix generated by the Kalman filter algorithms.

Table I

Initial Estimated Covariance Matrices

(1) MSFN E Matrix (see Note)

.680					
-.857	1.44				
.548	-.899	9.22		(Symmetric)	
.912	-.992	.842	1.70		
-.999	.854	-.540	-.908	.361	
.342	-.218	.088	.255	-.319	1.49

RSS 9.36 kft 2.29 fps

(2) Diagonal MSFN E (see Note)

.680					
	1.44				
		9.22			
			1.70		
(diagonal)				.361	
					1.49

RSS 9.36 kft 2.29 fps

(3) Scalar Diagonal MSFN E (same RSS) (see Note)

5.40					
	5.40				
		5.40			
			1.32		
(diagonal)				1.32	
					1.32

RSS 9.36 kft 2.29 fps

NOTE: Diagonal elements are standard deviations; off-diagonal elements are correlation coefficients. The RSS errors are position and velocity respectively.

(4) 2X Scalar Diagonal MSFN E (see Note)

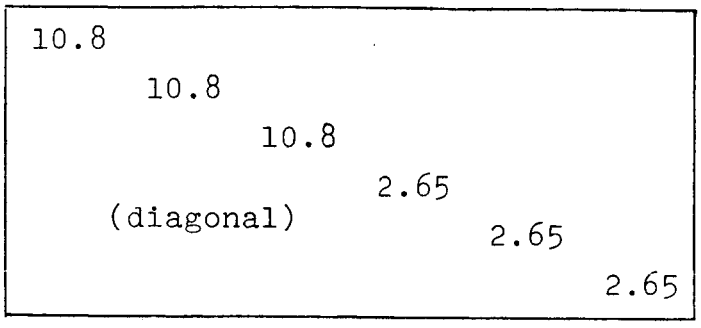

RSS 18.73 kft 4.59 fps

Table II

Sensor 1-sigma Random Errors Used in the Analysis

	VHF[4]	SXT[6]	RR (PNGCS)[7]
Range Error (ft)	80.	-----	500.
Range Scale Factor Error (%)	-----	-----	.33
Range Rate Error (ft/sec)	-----	-----	1.
Range Rate Scale Factor Error (%)	-----	-----	.4
Angle Error (mr)	-----	.2	5.

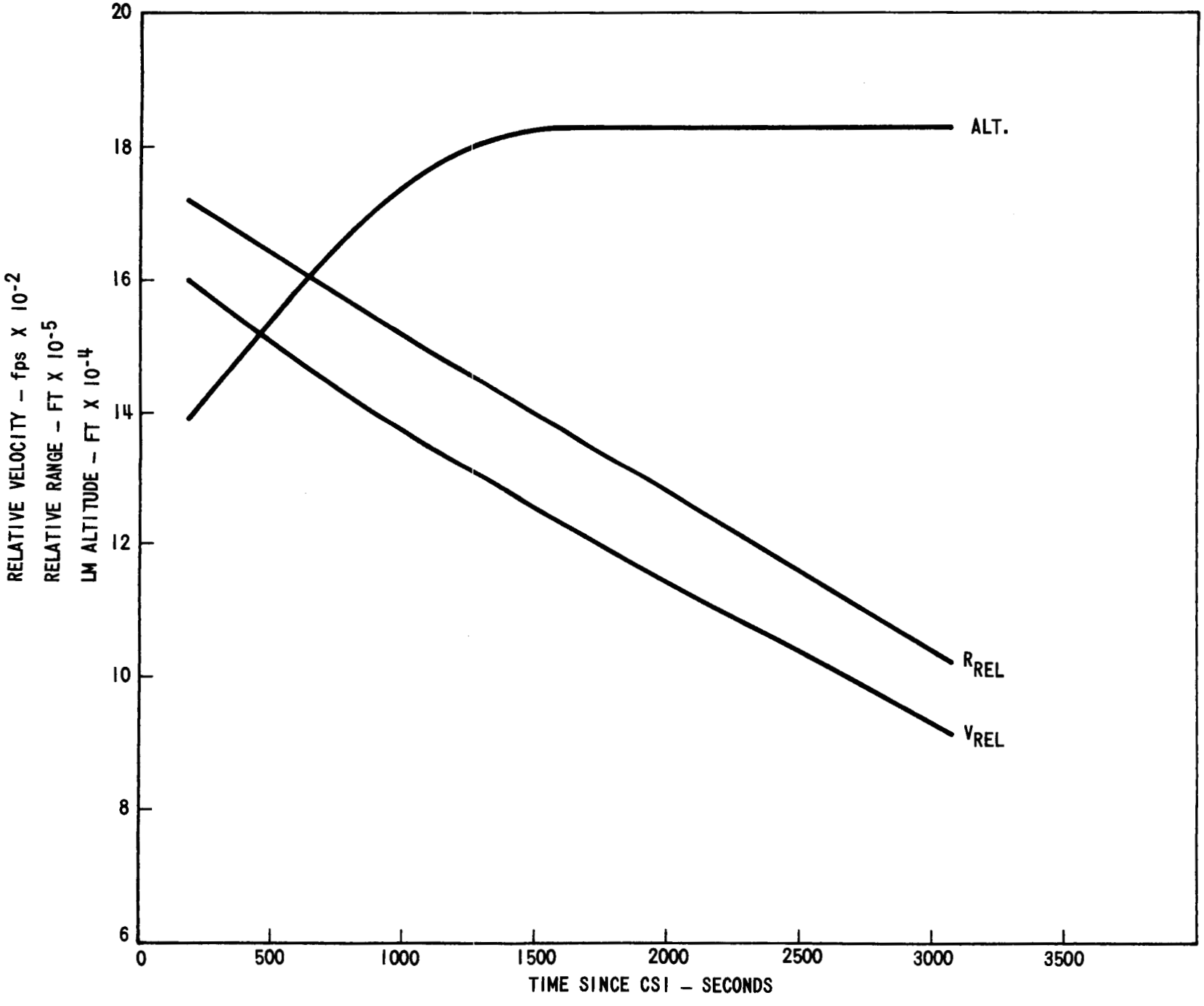

FIGURE 1. LM ALTITUDE AND RELATIVE POSITION AND VELOCITY

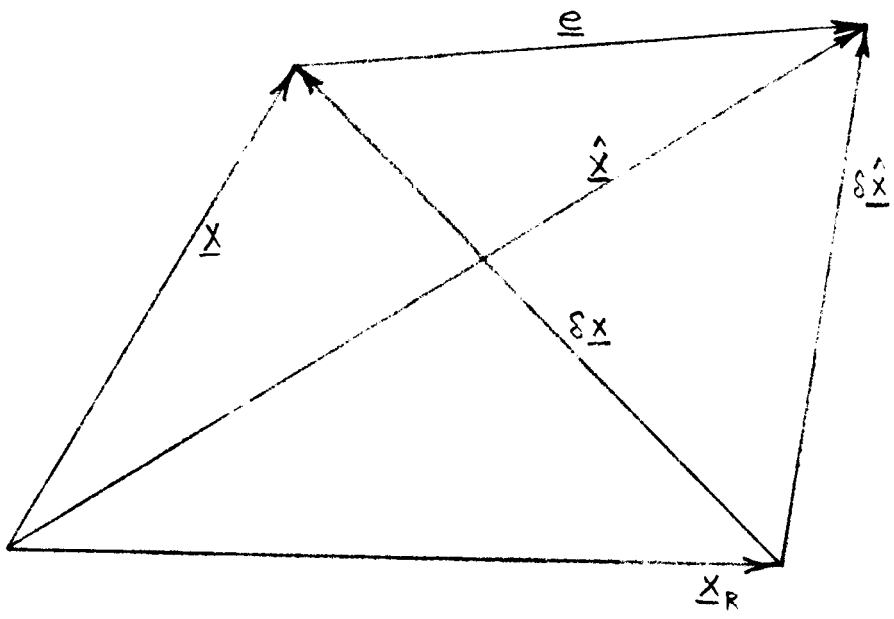

$\underline{X}_R$ = reference state vector

$\underline{X}$ = actual state vector

$\hat{\underline{X}}$ = estimated state vector

$\delta\underline{X}$ = deviation vector

$\delta\hat{\underline{X}}$ = estimate deviation vector

$\underline{e}$ = navigation error

FIGURE 2

Definition of State Vectors and Navigation Error

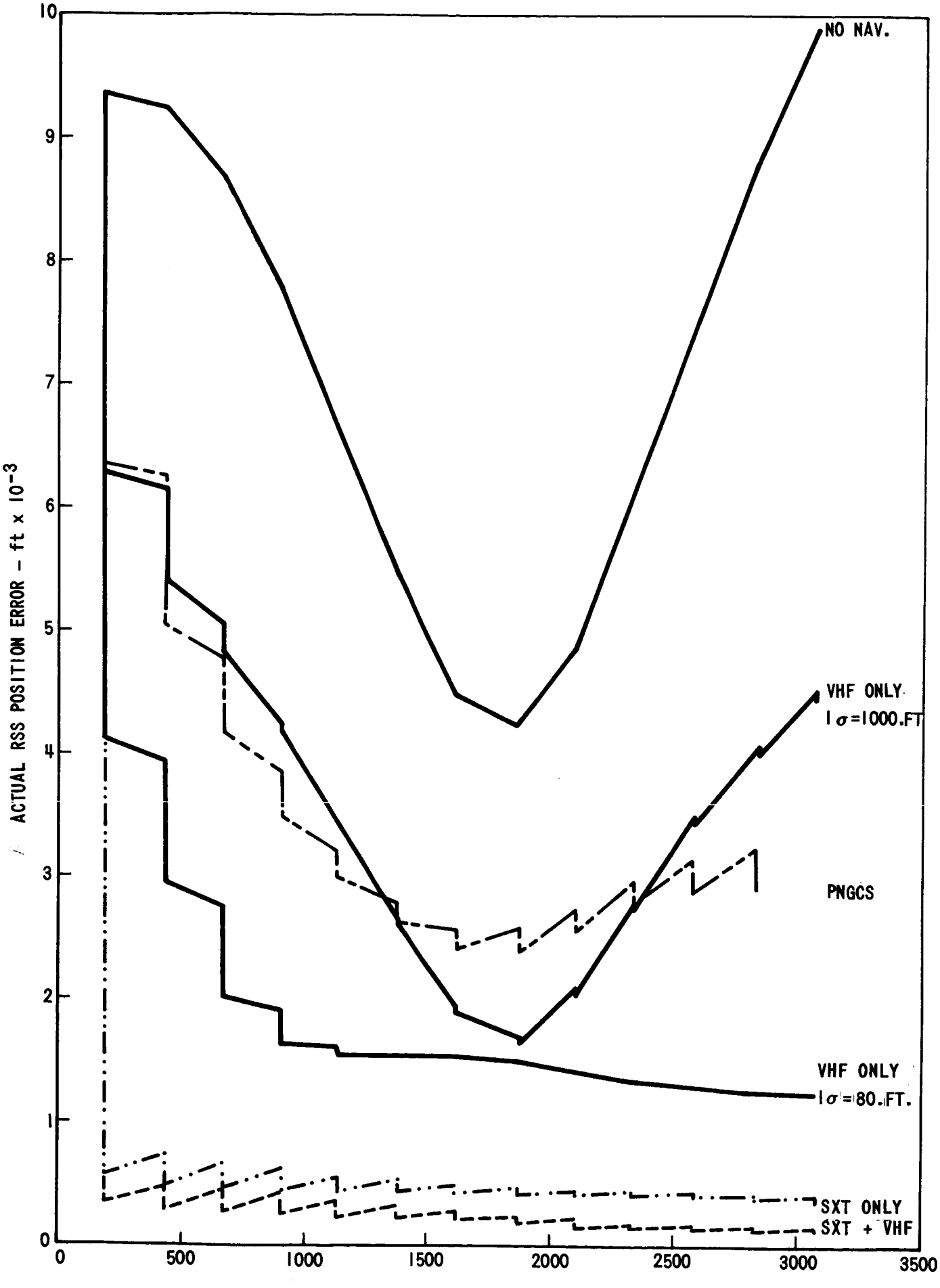

FIGURE 3. RSS POSITION ERROR FOR MSFN E

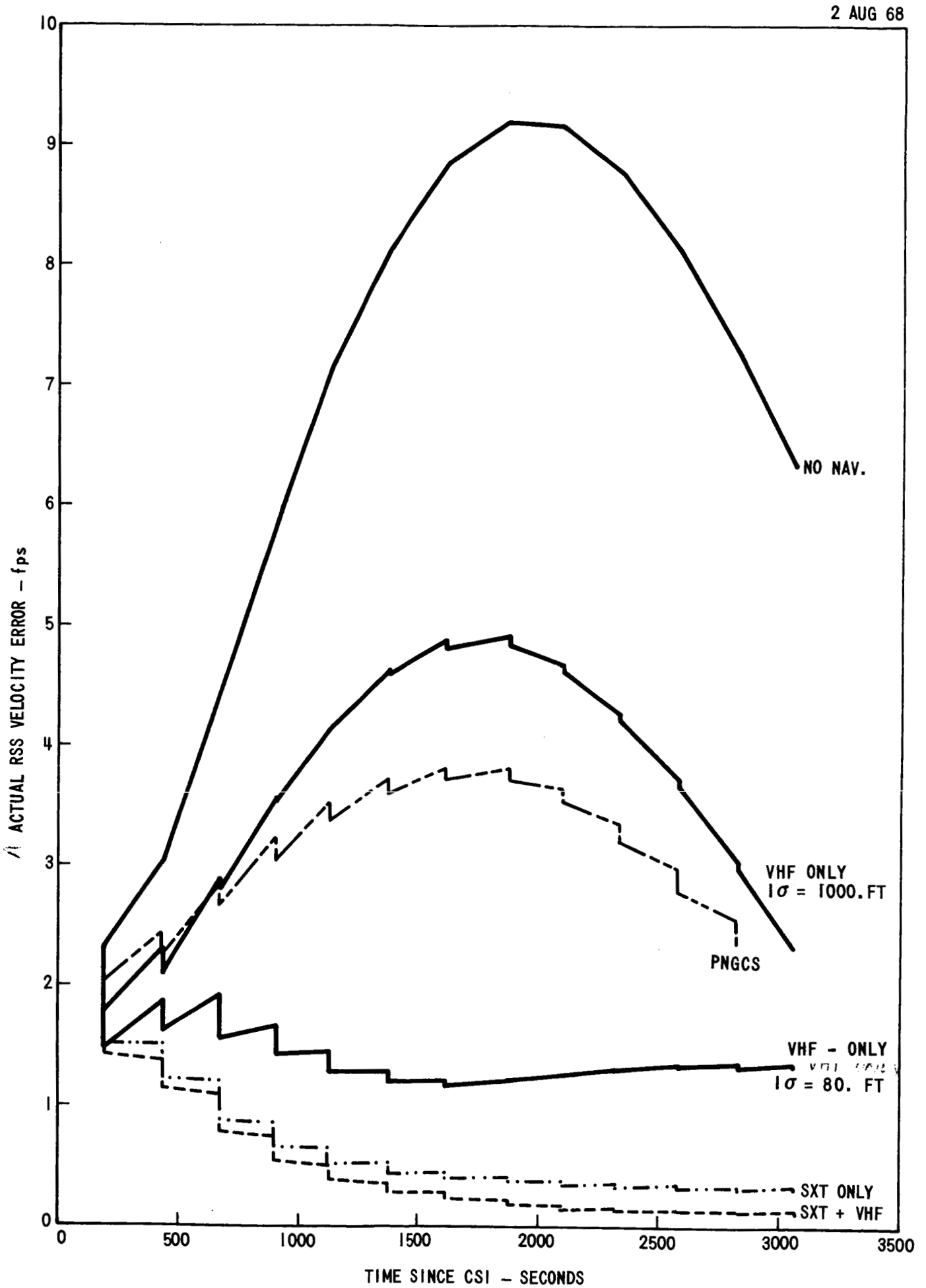

FIGURE 4. RSS VELOCITY ERROR FOR MSFN E

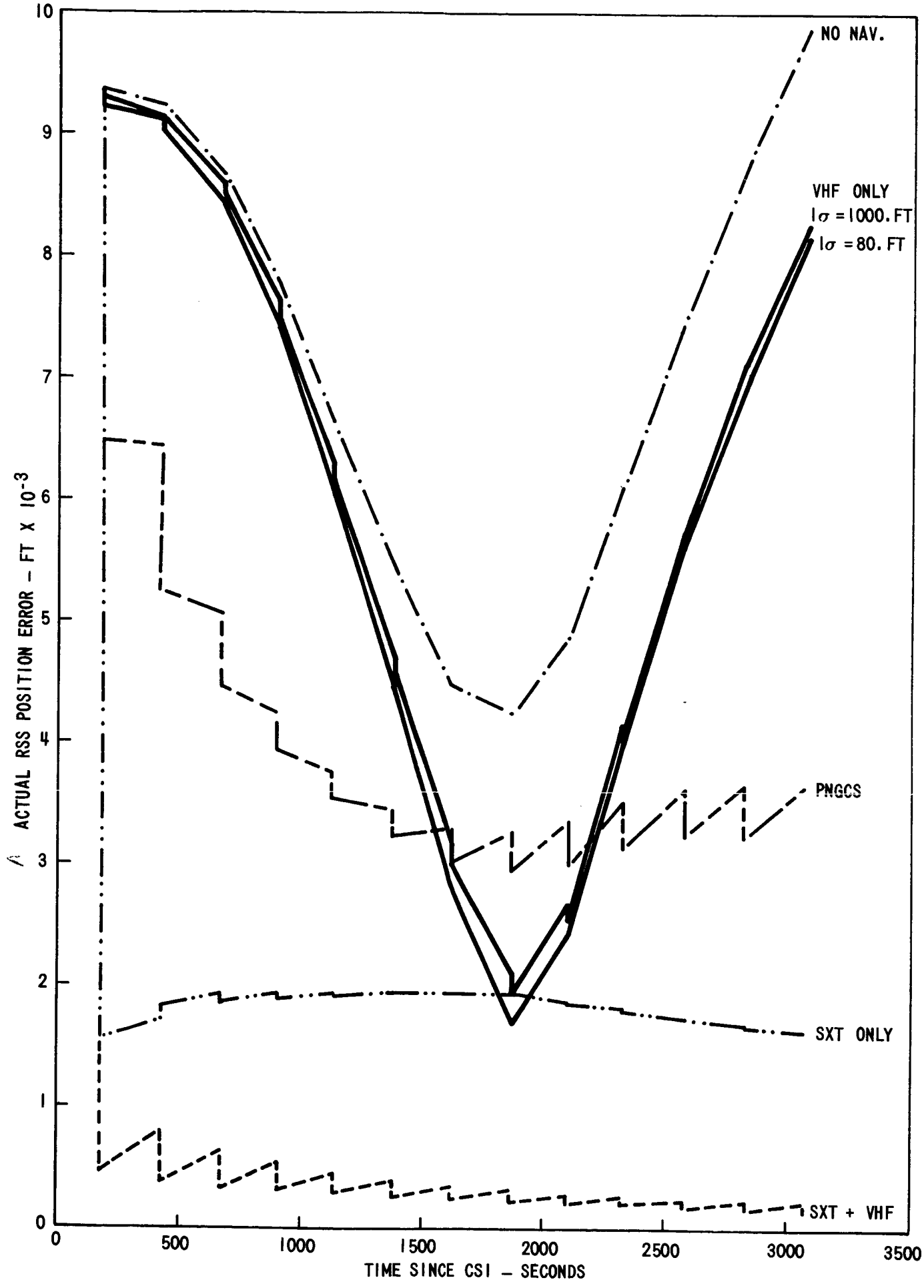

FIGURE 5. RSS POSITION ERROR FOR DIAGONAL E

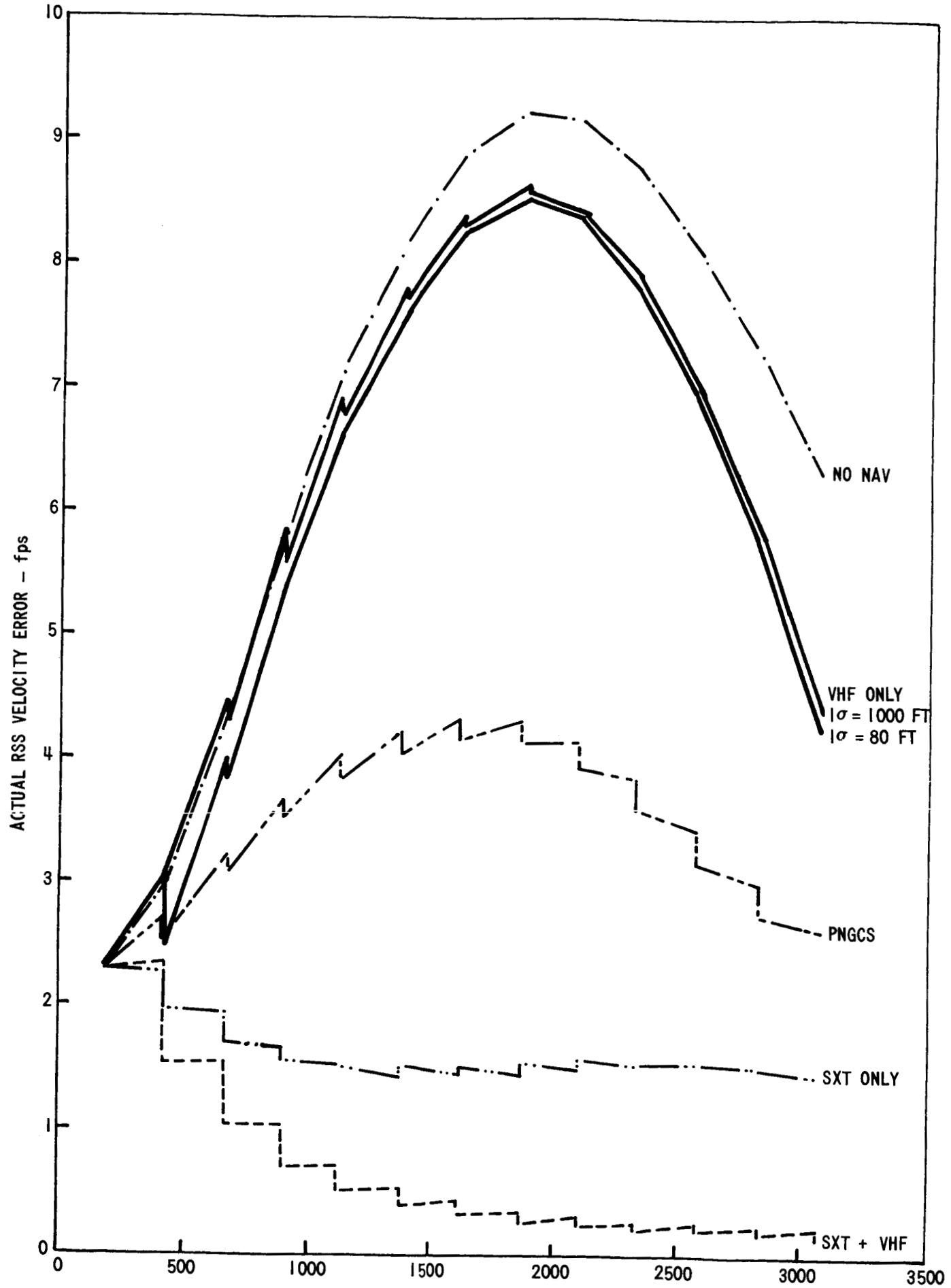

FIGURE 6. RSS VELOCITY ERROR FOR DIAGONAL E

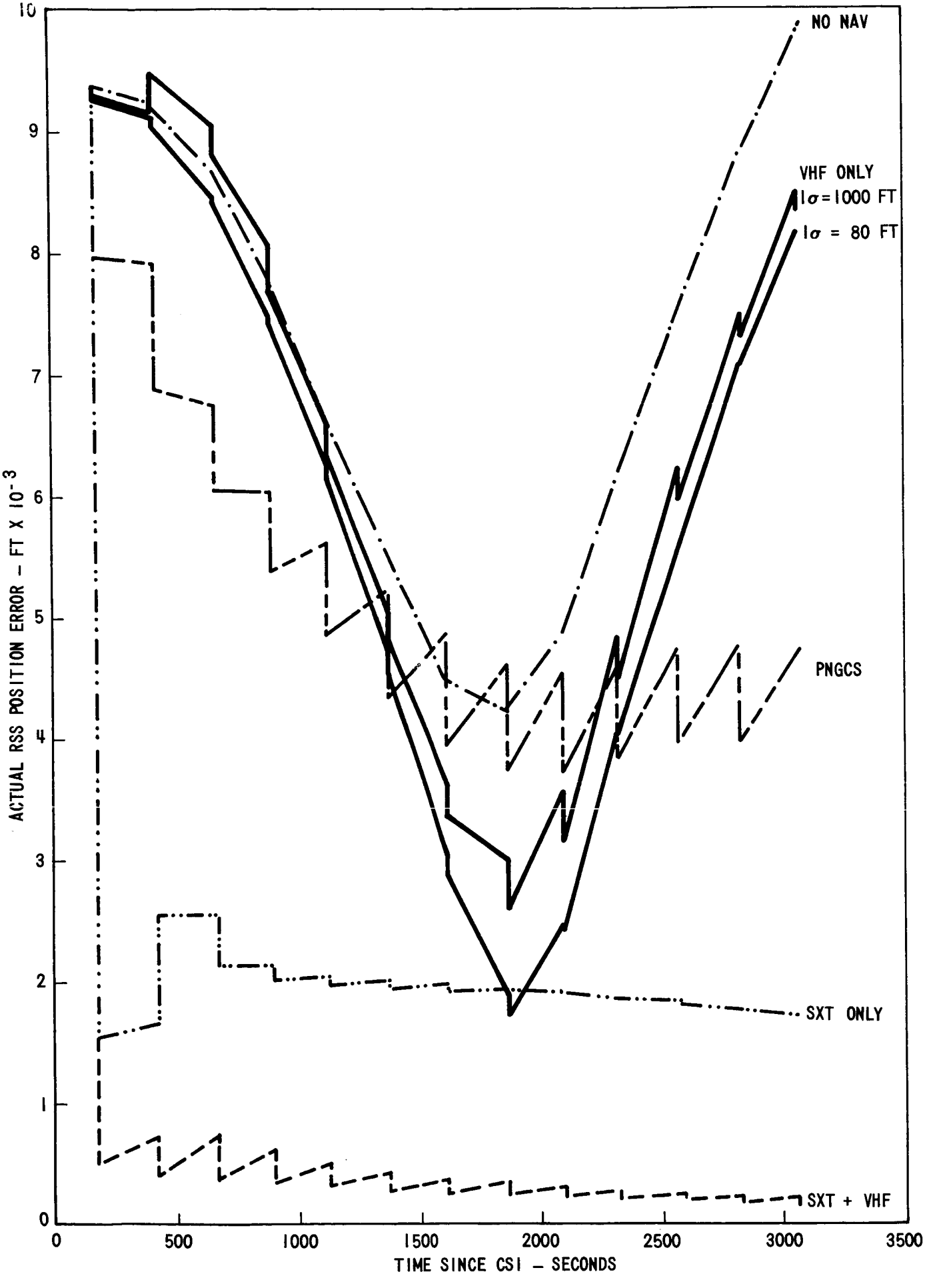

FIGURE 7. RSS POSITION ERROR FOR SCALAR DIAGONAL E

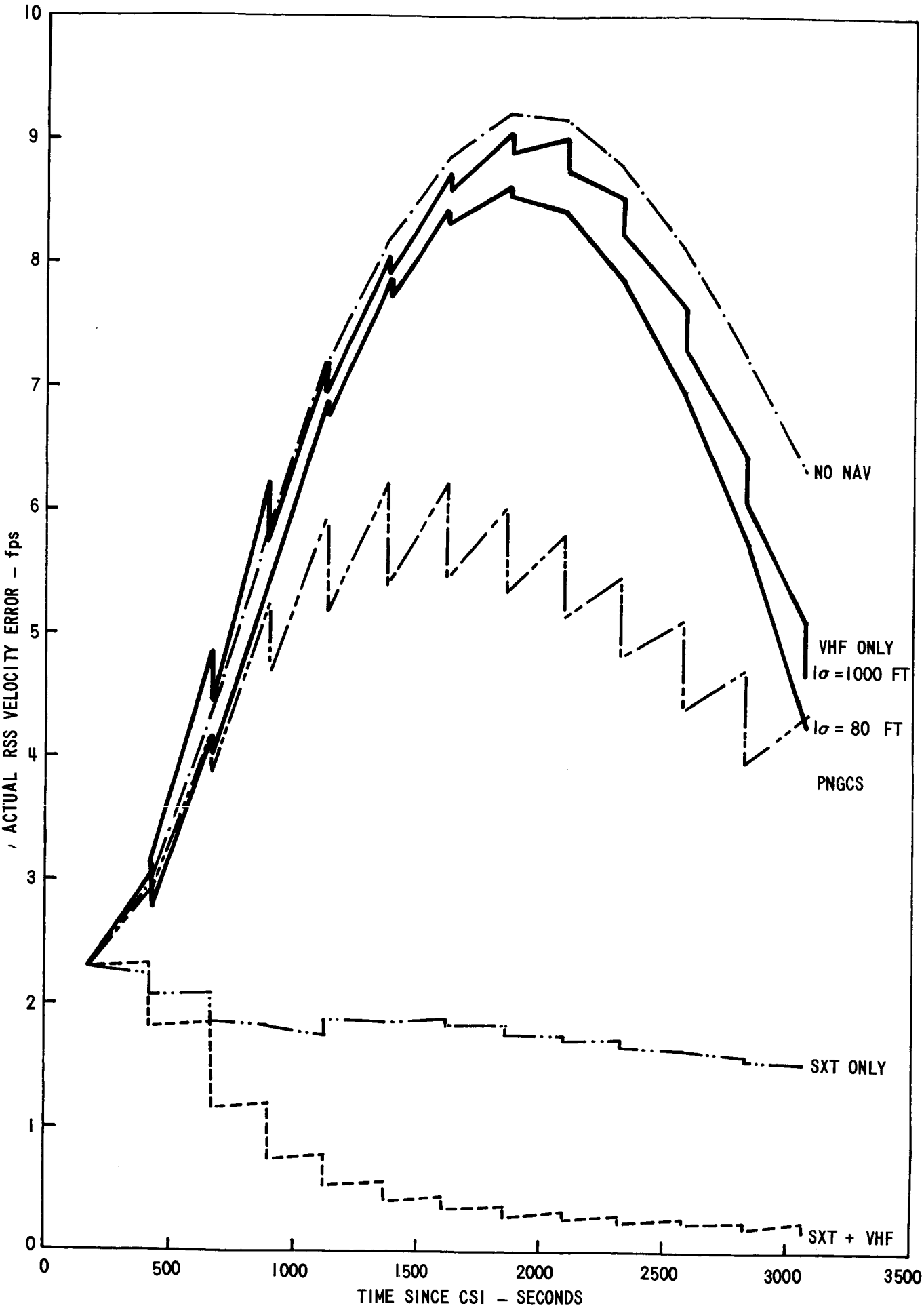

FIGURE 8. RSS VELOCITY ERROR FOR SCALAR DIAGONAL E

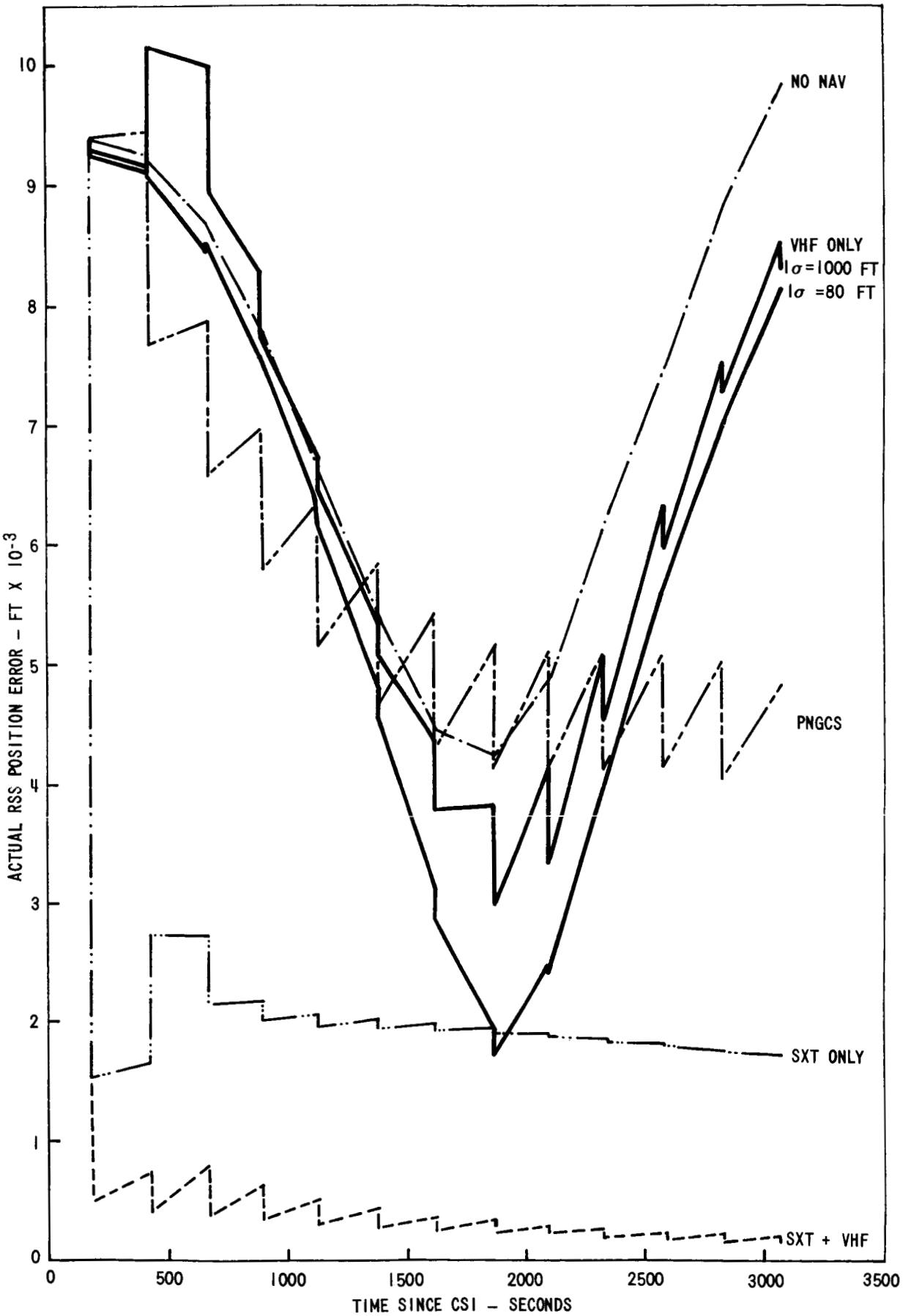

FIGURE 9. RSS POSITION ERROR FOR SCALAR DIAGONAL E = 2 X (MSFN E)

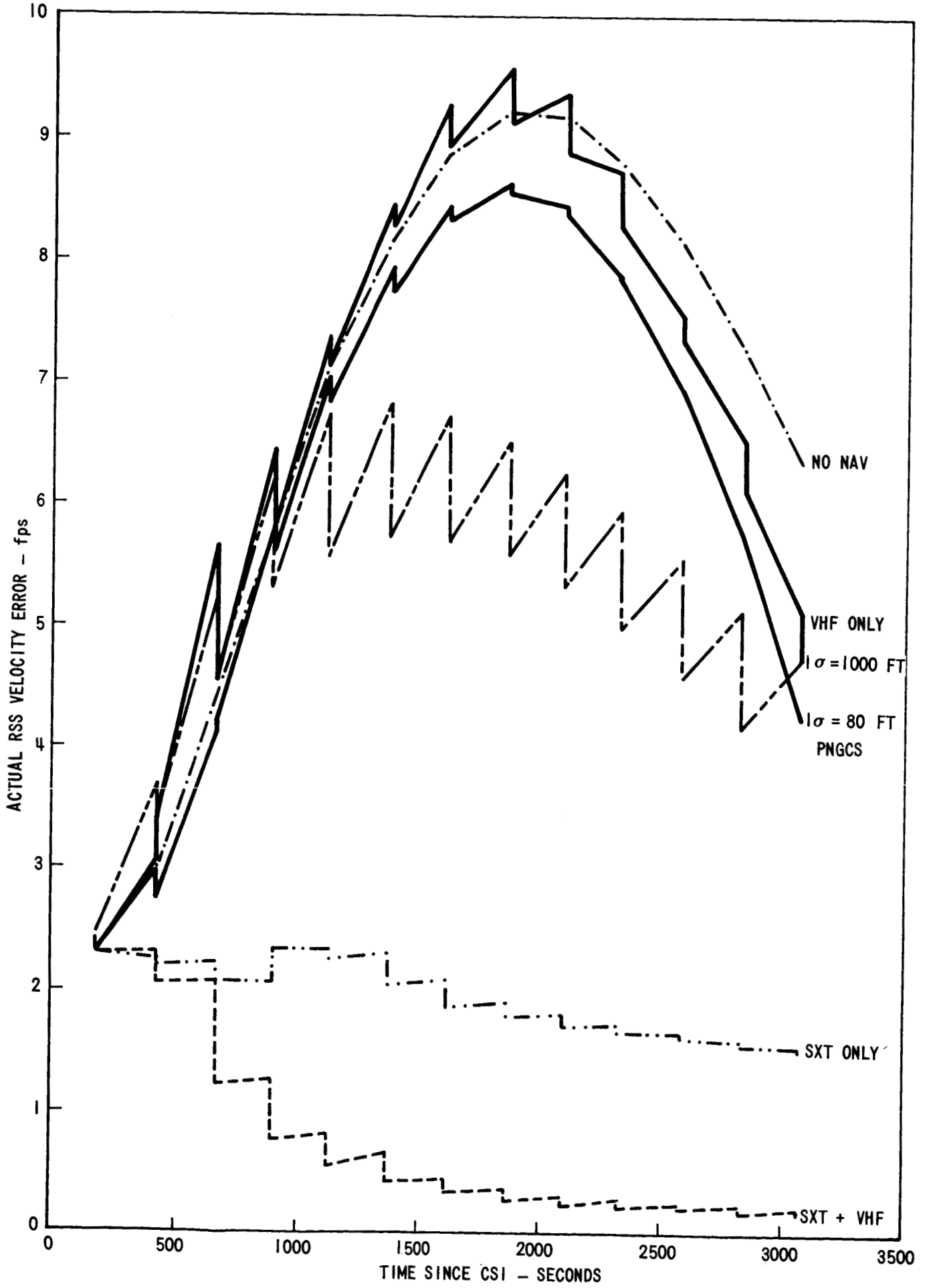

FIGURE 10. RSS VELOCITY ERROR FOR SCALAR DIAGONAL E = 2(MSFN E)

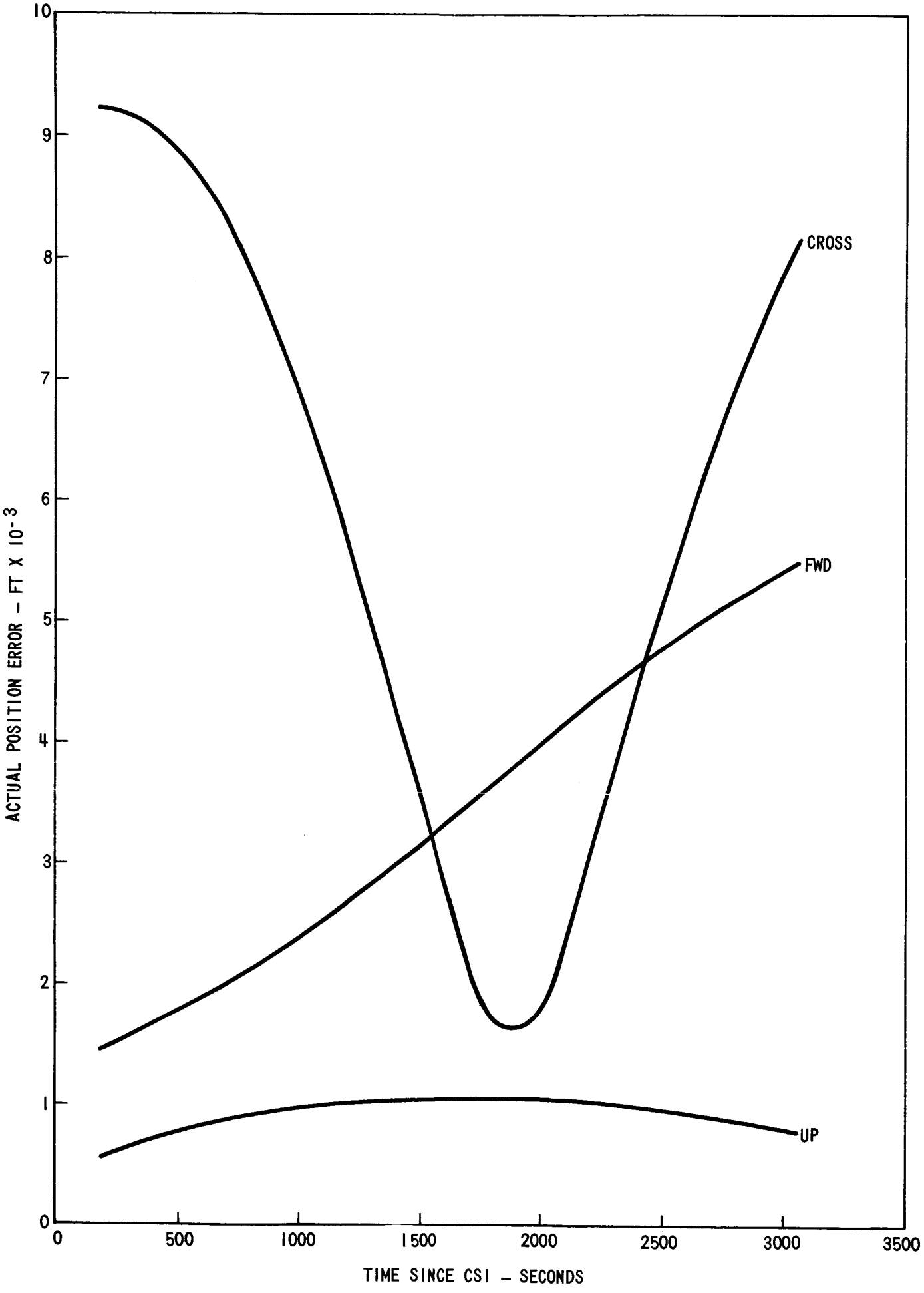

FIGURE 11. COMPONENTS OF POSITION ERROR, NO NAV

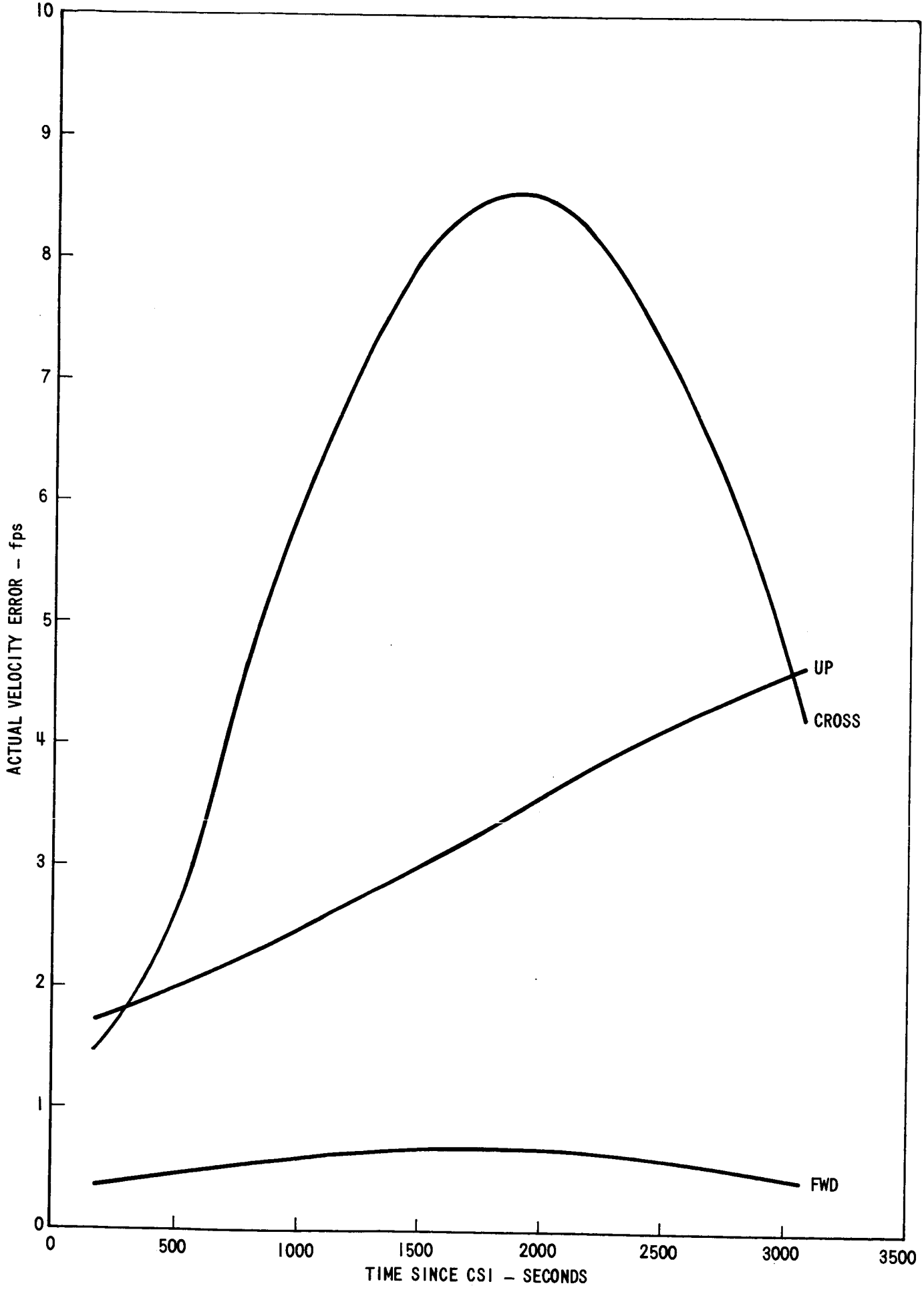

FIGURE 12. COMPONENTS OF VELOCITY ERROR, NO NAV

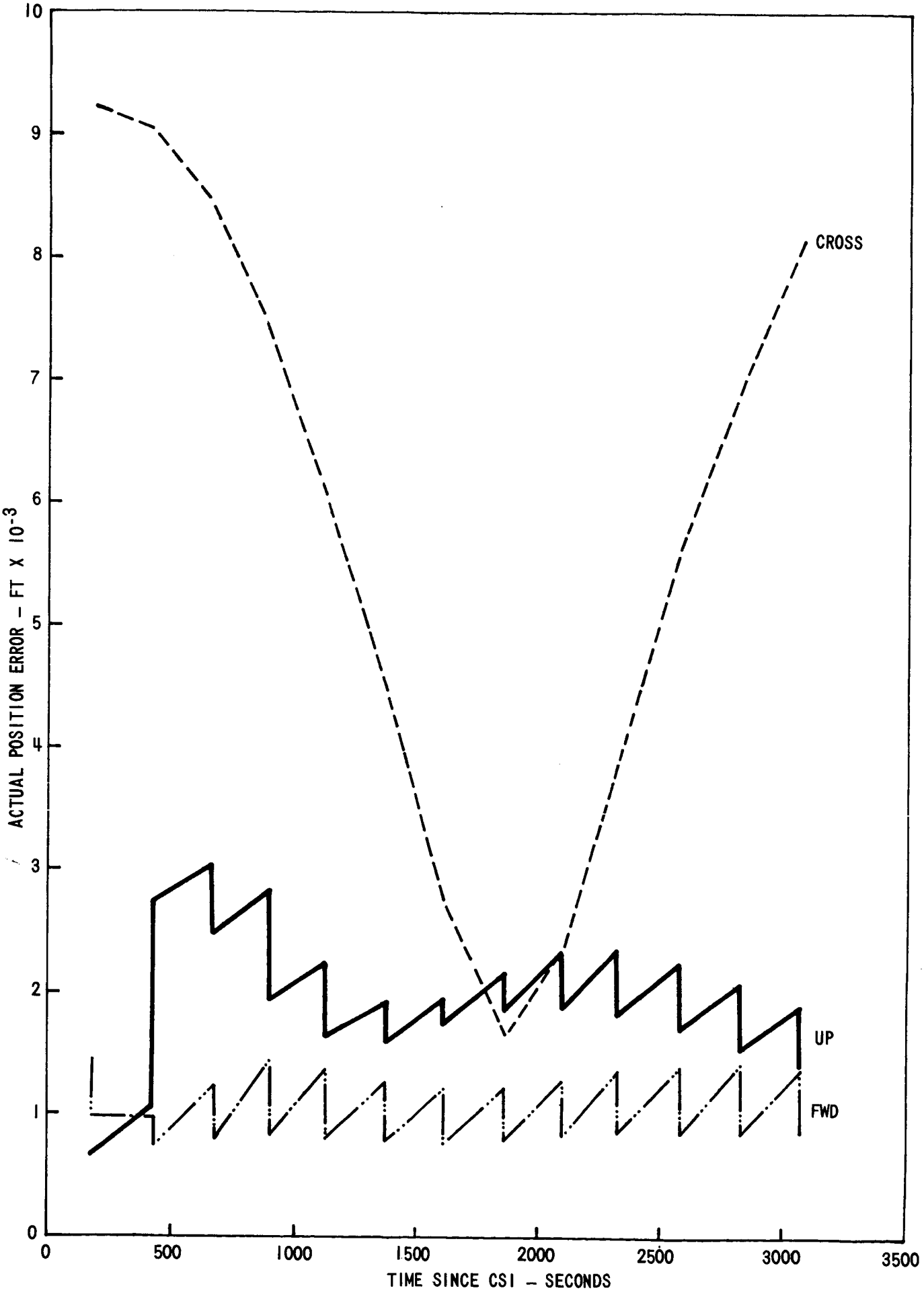

FIGURE 13. COMPONENTS OF POSITION ERROR, E = SCALAR EA
VHF ONLY, 1σ = 1000 FT

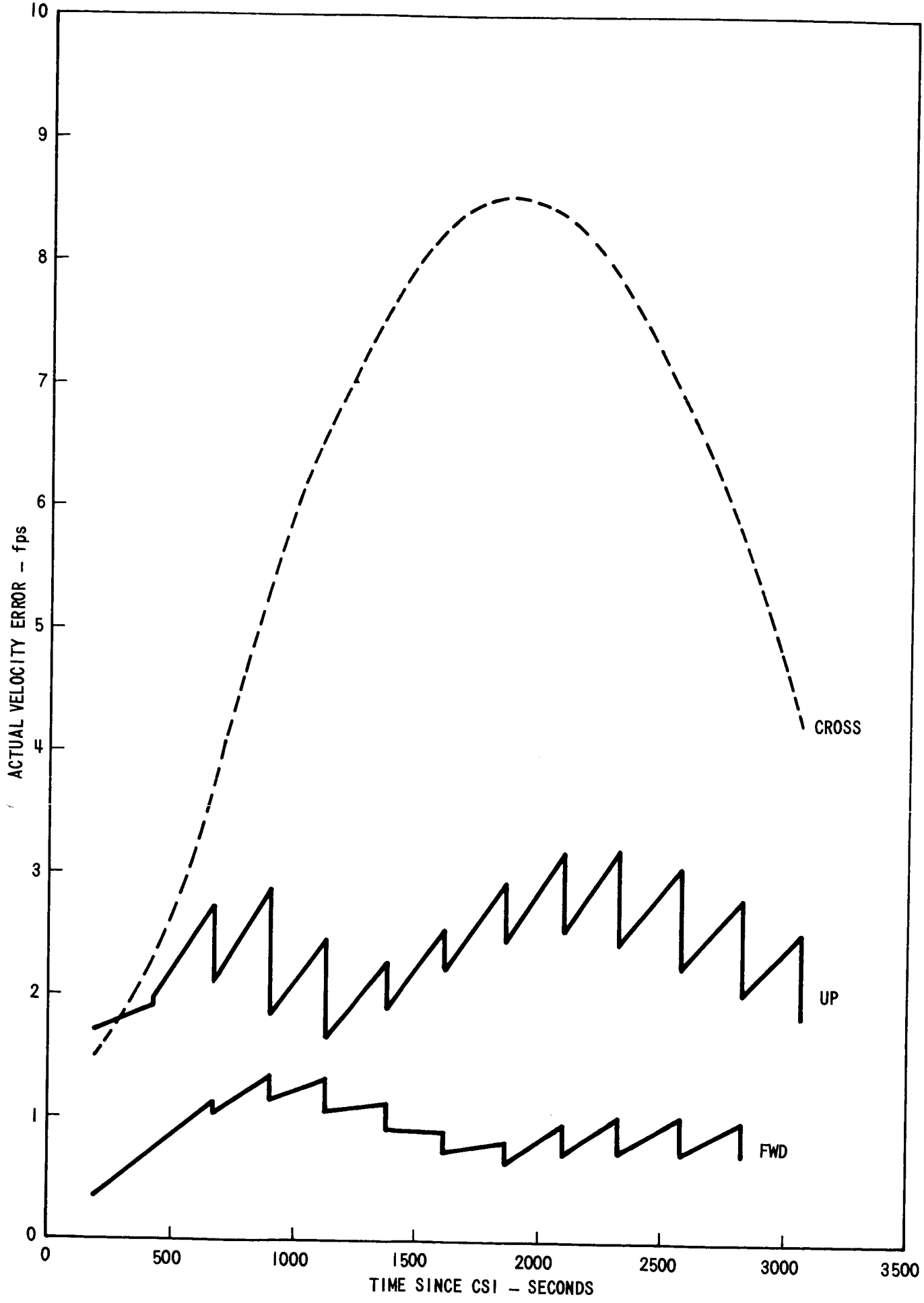

FIGURE 14. COMPONENTS OF VELOCITY ERROR, VHF ONLY 1σ = 1000 FT E = SCALAR EA

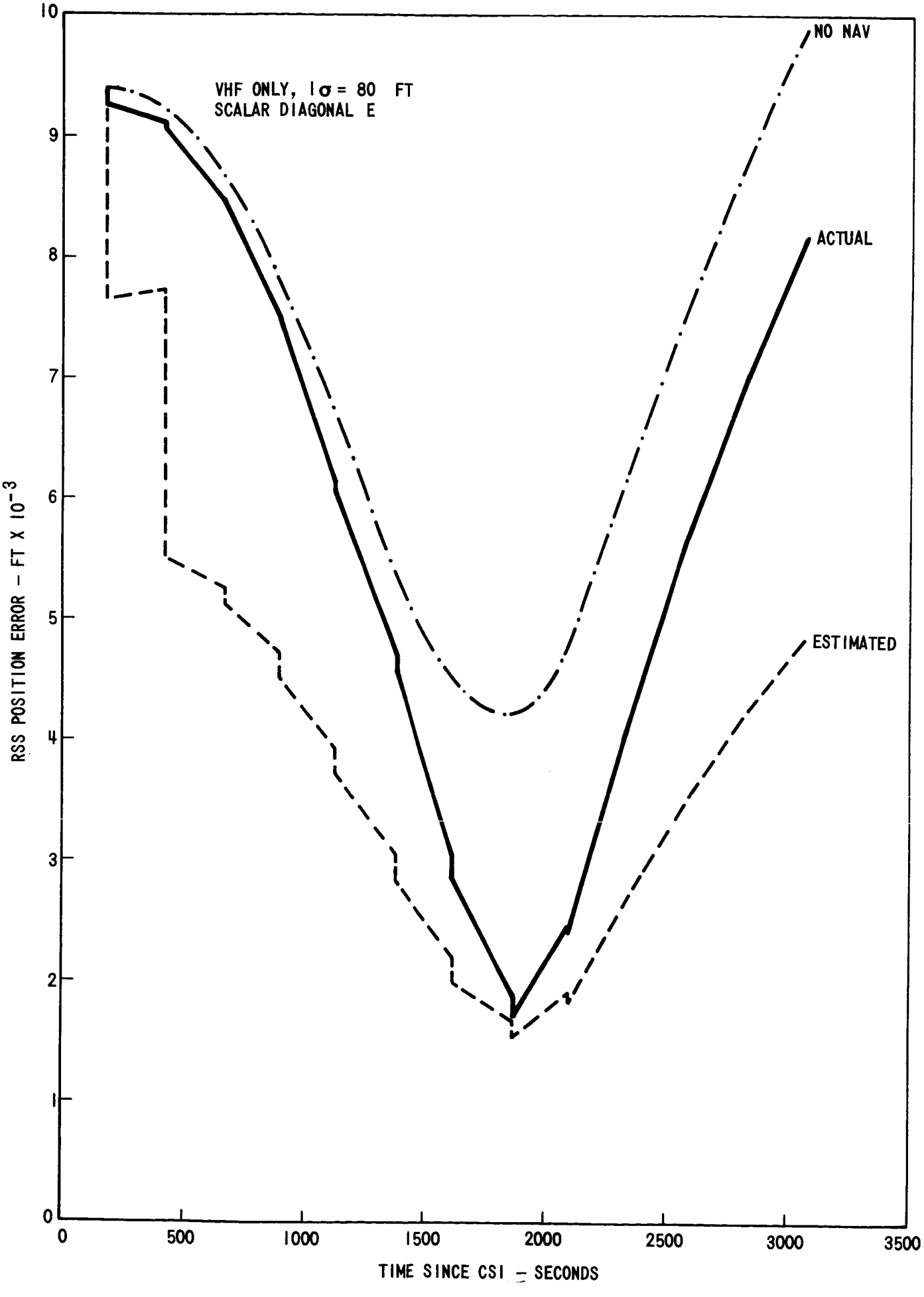

FIGURE 15. COMPARISON OF ACTUAL & ESTIMATED RSS POSITION ERROR

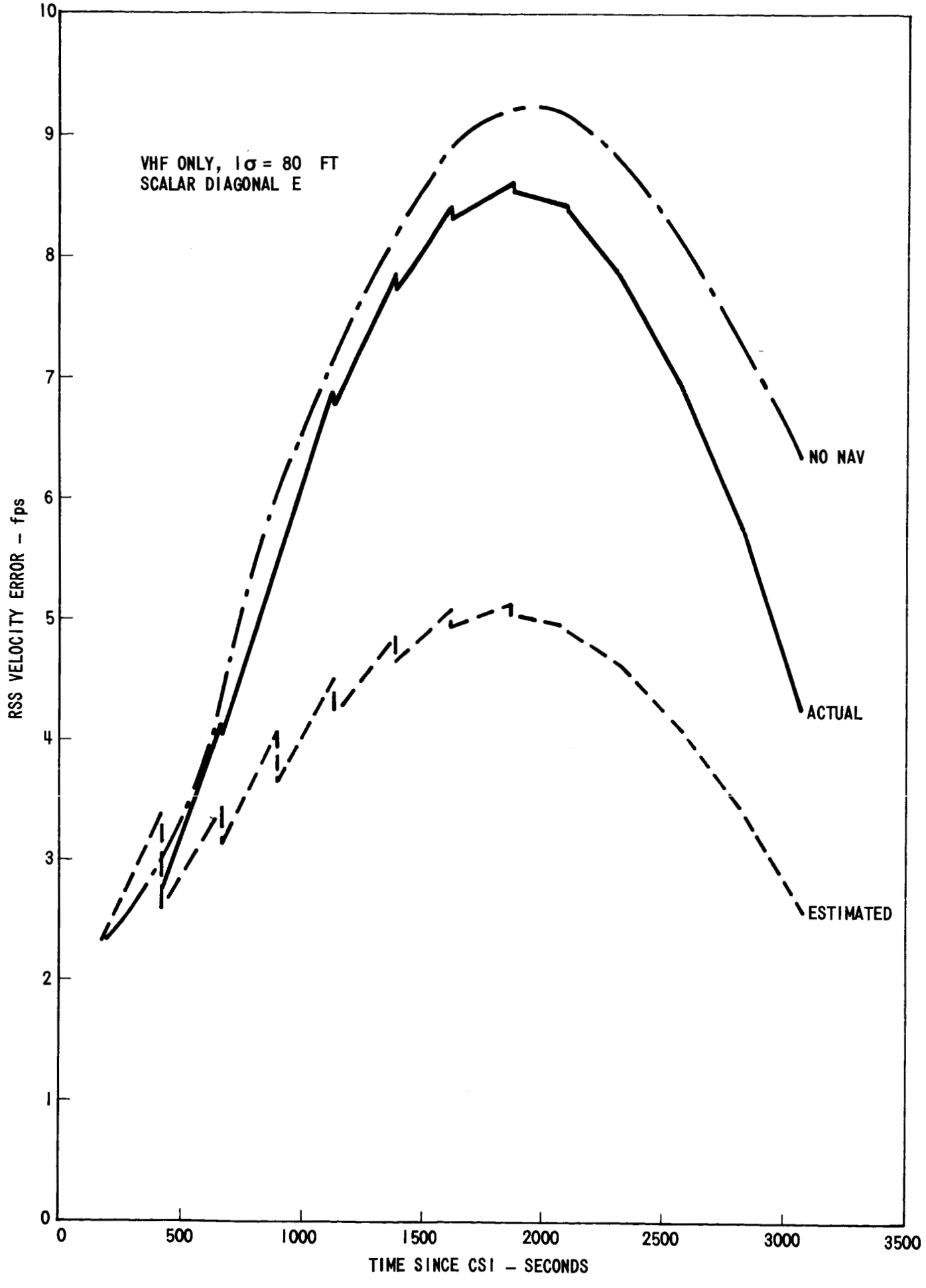

FIGURE 16. COMPARISON OF ACTUAL & ESTIMATED RSS VELOCITY ERROR

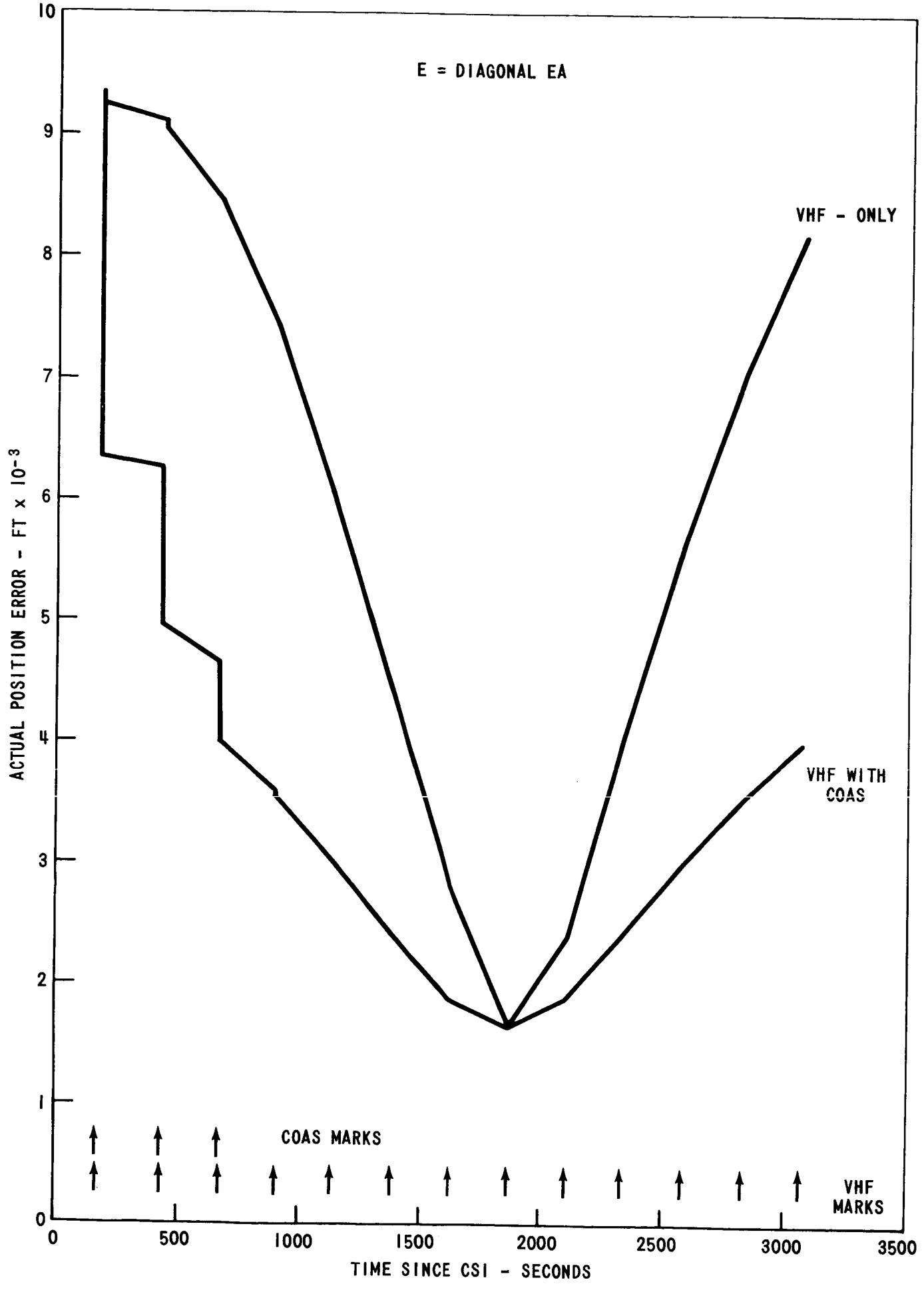

FIGURE 17. VHF POSITION ERROR IMPROVEMENT WITH COAS

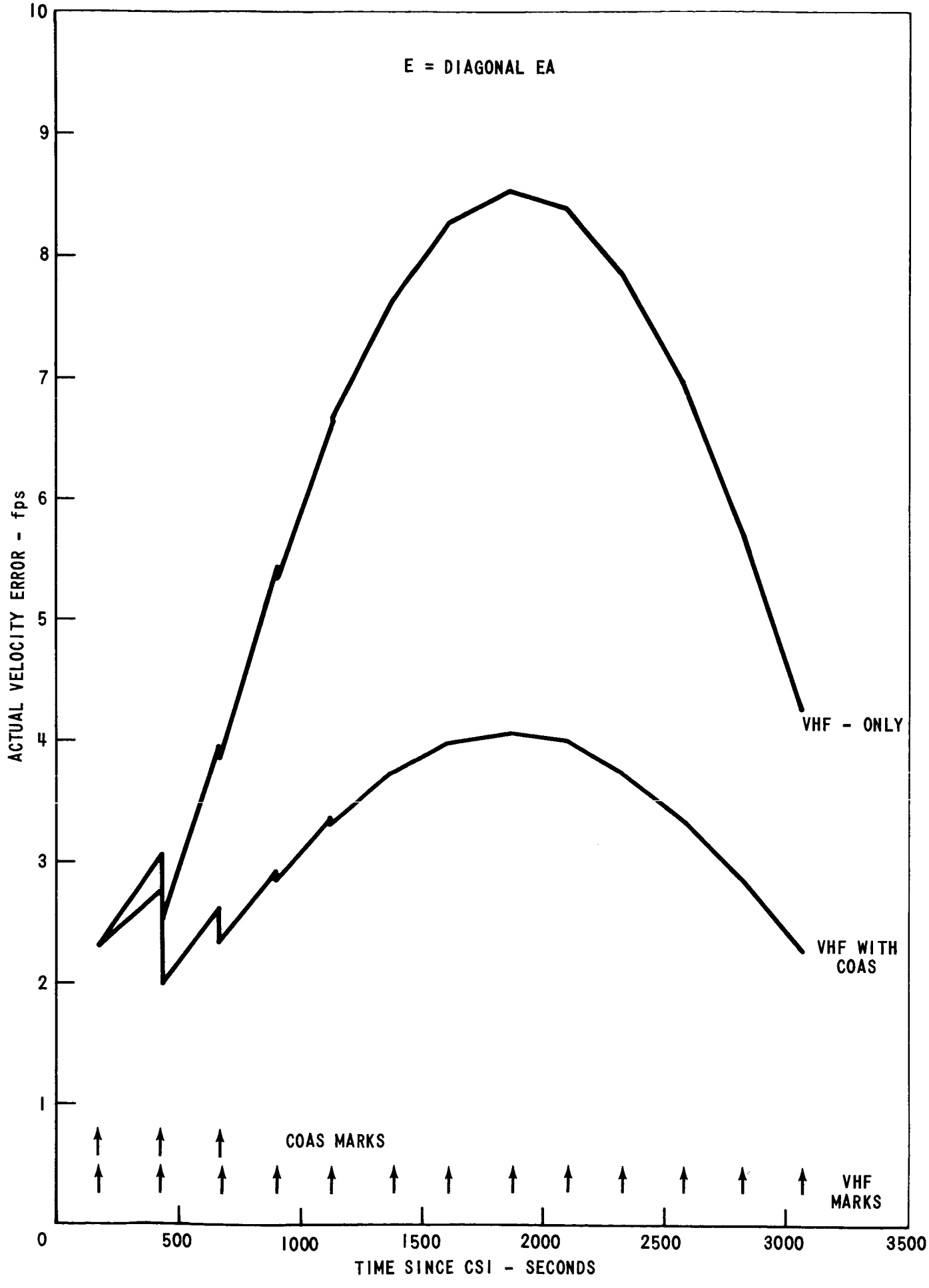

FIGURE 18. VHF VELOCITY ERROR IMPROVEMENT WITH COAS

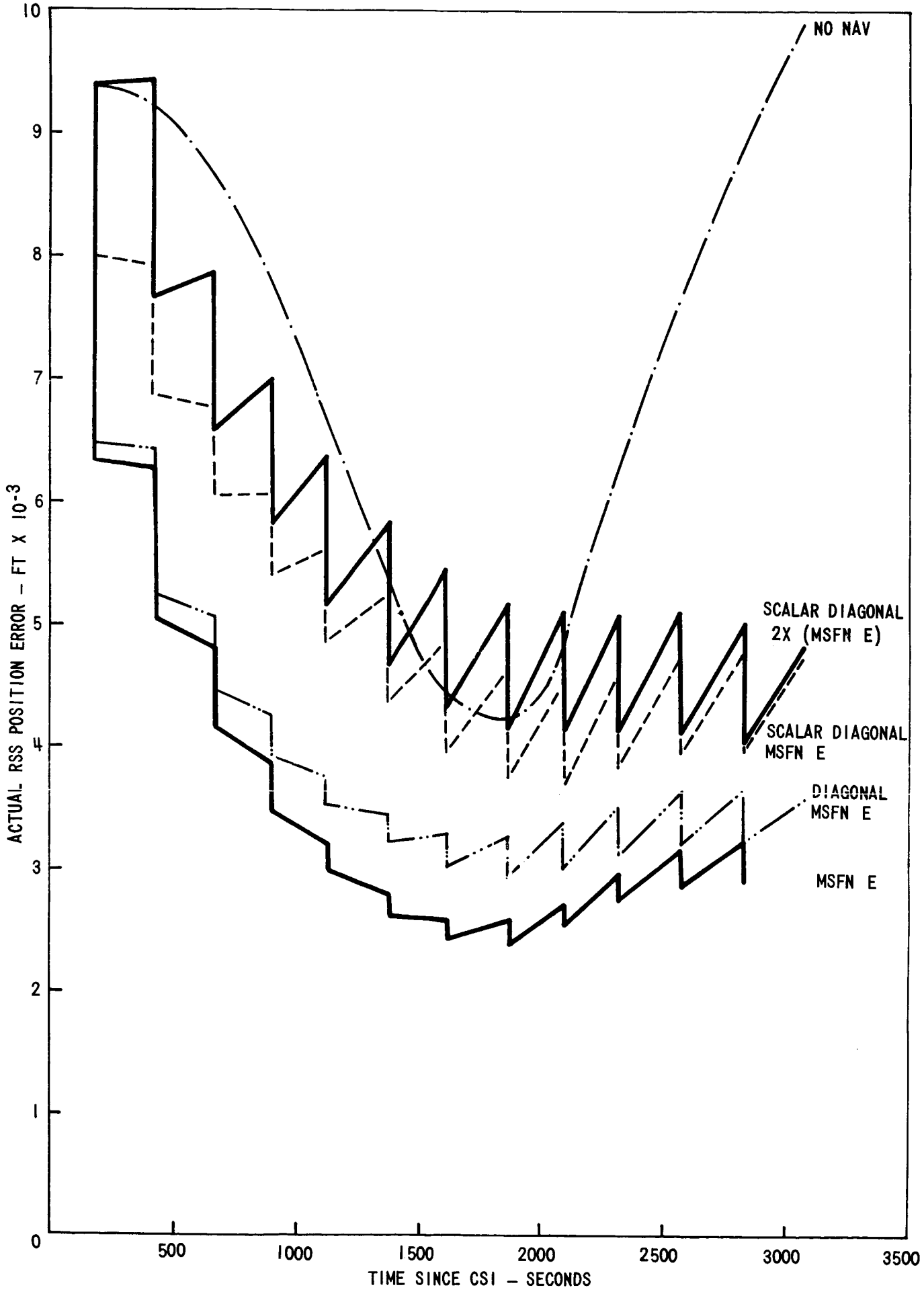

FIGURE 19. EFFECT OF INITIAL E ON POSITION ERROR, PNGCS

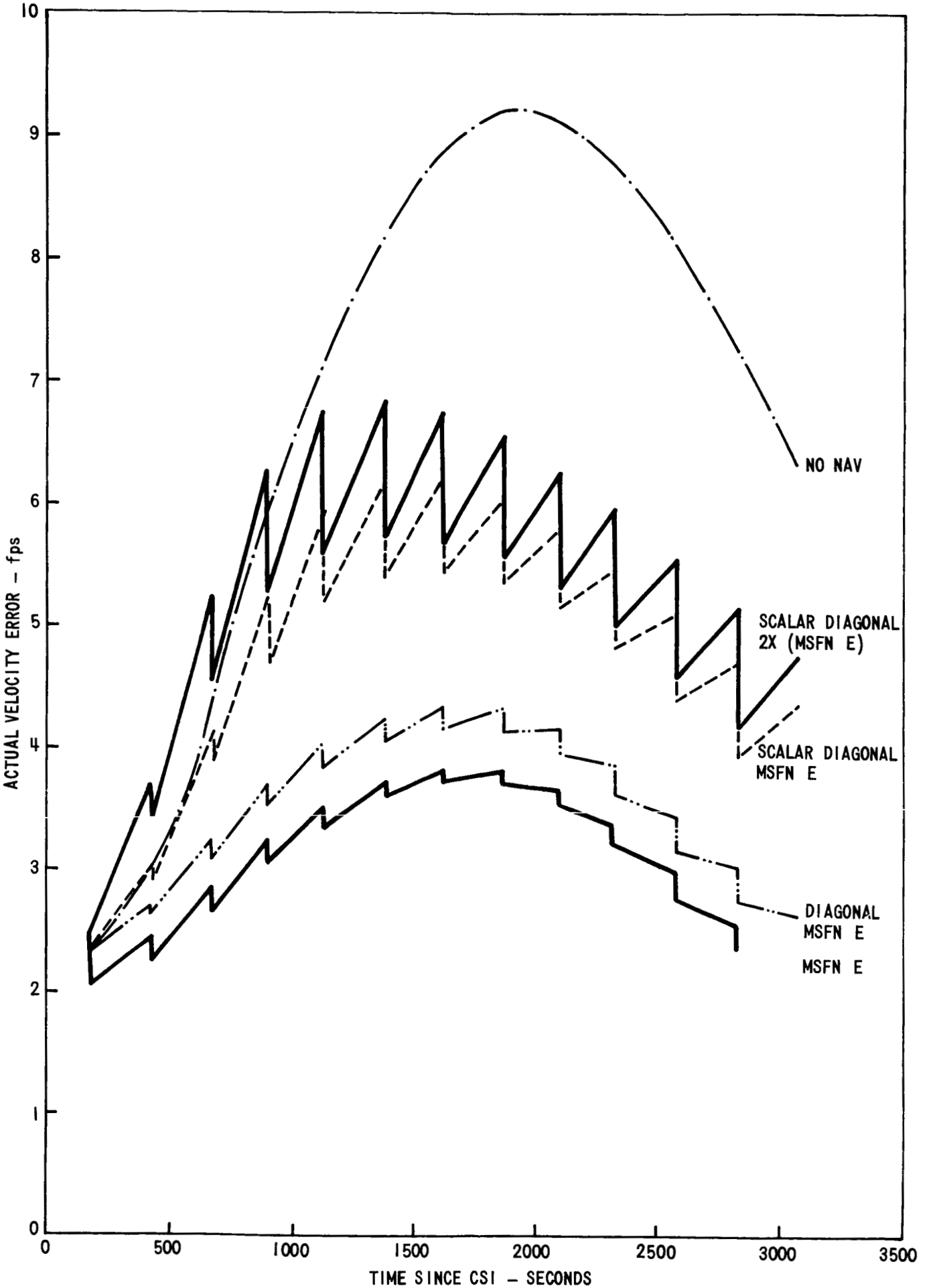

FIGURE 20. EFFECT OF INITIAL E ON VELOCITY ERROR, PNGCS

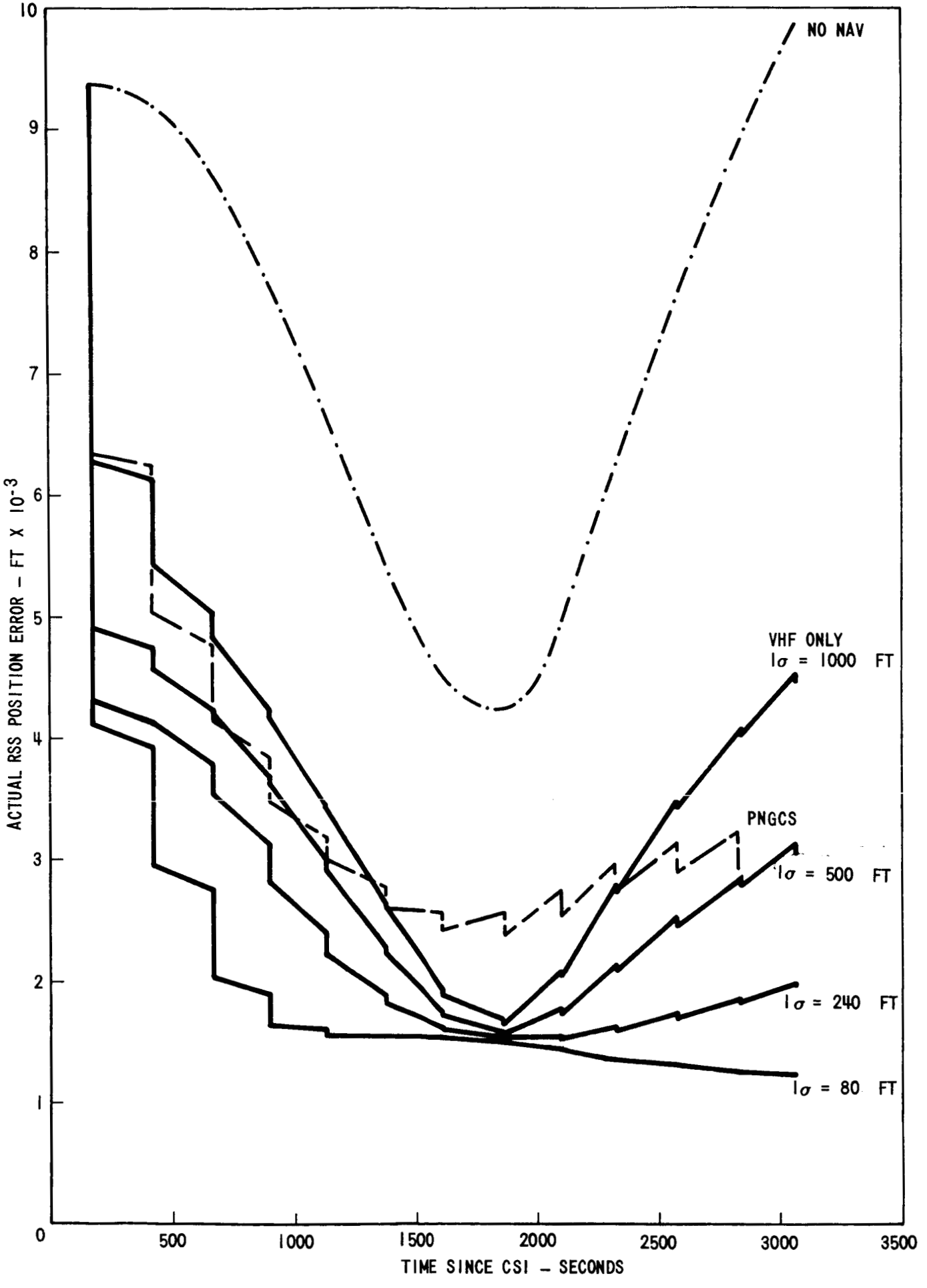

FIGURE 21. EFFECT OF VHF PERFORMANCE ON RSS POSITION ERROR FOR MSFN E

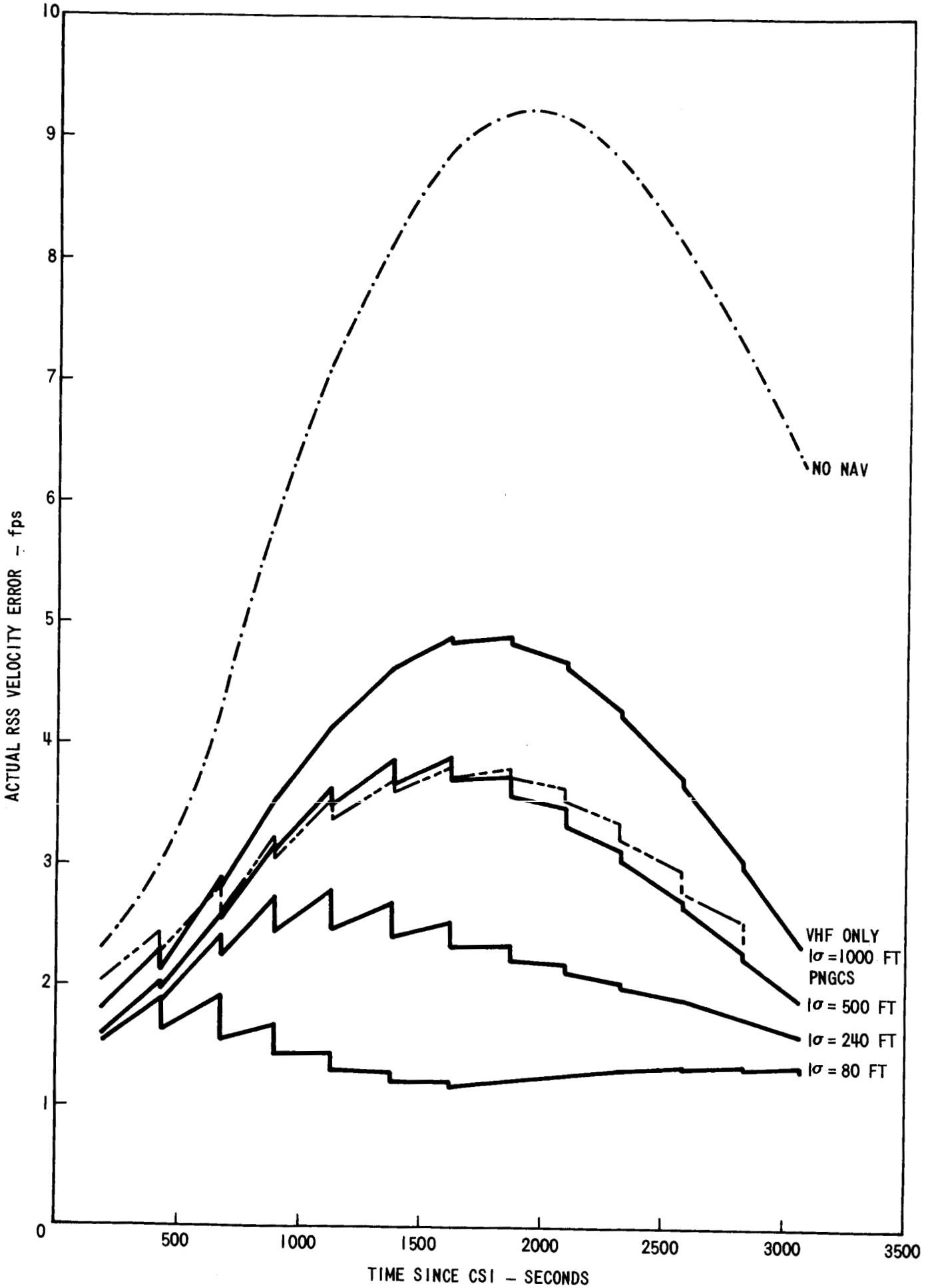

FIGURE 22. EFFECT OF VHF PERFORMANCE ON RSS VELOCITY ERROR FOR MSFN E